Journal of Sound and Vibration (2002) **254**(4), 805–817
doi:10.1006/jsvi.2001.3972, available online at http://www.idealibrary.com on IDEAL®

ON THE ORTHOGONAL WAVELET TRANSFORM FOR MODEL REDUCTION/SYNTHESIS OF STRUCTURES

M. Al-Aghbari, F. Scarpa and W. J. Staszewski

*Department of Mechanical Engineering, University of Sheffield, Sheffield S*1 3*JO, England.*
E-mail: w.j.staszewski@sheffield.ac.uk

(*Received* 21 *June* 2001, *and in final form* 24 *July* 2001)

1. INTRODUCTION

Model reduction techniques are widely used in numerical structural dynamics to synthesize large matrix systems and perform fast computations of natural frequencies and mode shapes. Several new model reduction techniques have been proposed in recent years. Methods such as the Guyan (or static) reduction, dynamic condensation, the improved reduced system (IRS) approach or the system equivalent reduction expansion (SEREP) may be used with good results, especially over low-frequency ranges [1–5]. While the Guyan is based solely on the stiffness matrix reduction, the SEREP has been shown to map exactly the mass and stiffness matrices for a desired set of modes at an arbitrary set of d.o.f. using a dynamic condensation technique with the full modal basis of the system. On the other hand, the IRS uses Guyan reduction as an estimate of the reduction system and then makes adjustments to compensate for the inertia effects that were ignored in the Guyan process, without the penalty of requiring a full eigensolution. Advantages of using these techniques are their relative efficiency and cost effectiveness when compared with analysis on the full system model. A disadvantage, however, is the approximate system descriptions that result from their use, sometimes leading to serious error. Such methods also require skilled selection of the number and location of the reduced degrees of freedom that can make up the reduced system. If the degrees of freedom that represent the reduced system are chosen improperly, poor solution results will follow [4]. Moreover, classical model reduction techniques are not appropriate for synthesizing the dynamic behaviour of structures in the middle- and high-frequency range, or with high modal densities. This fact leads the structural analyst to prepare large numerical (FEM) models with high computational costs or to use statistical energy analysis (SEA) methods to predict the dynamic behaviour of the structure for high-frequency ranges. On the other hand, large finite element models are already prepared for static analysis purposes. Their lack of use for dynamic analysis leads to an increase of the global pre-processing time which greatly consumes manpower resources. The existence of a reliable condensation technique for structural middle and high frequencies would also speed up the evaluation of novel materials and structures concepts for aerospace and naval applications [6].

The aim of this paper is to explore the orthogonal wavelet transform for model synthesis of structures in order to preserve the middle- and high-frequency spectra components only. A new technique is illustrated using two simple simulated examples, namely a simply supported beam and a framework structure. The technique is intended as an initial step

0022-460X/02/$35.00

towards a more comprehensive condensation method for numerical structural models in the frequency ranges where classical condensation techniques fail to achieve the degree of accuracy desired.

2. MODEL REDUCTION BASED ON WAVELET COMPRESSION

For an undamped m.d.o.f. system, with N degrees of freedom, the governing equations of motion can be written in matrix form as

$$[\mathbf{M}]\{\mathbf{x}(t)\} + [\mathbf{K}]\{\mathbf{x}(t)\} = \{\mathbf{f}(t)\}, \tag{1}$$

where $[\mathbf{M}]$ and $[\mathbf{K}]$ are $N \times N$ mass and stiffness matrices, respectively, $\{\mathbf{x}(t)\}$ and $\{\mathbf{f}(t)\}$ are $N \times 1$ vectors of time-varying displacements and forces respectively. The non-trivial solution of the above homogenous equation ($f = 0$) is obtained solving the characteristic equation

$$([\mathbf{K}] - \omega^2[\mathbf{M}])\{\mathbf{X}\} = \{\mathbf{0}\}. \tag{2}$$

The complete free vibration solution can be expressed by two $N \times N$ eigenmatrices

$$[\ddots\ \varpi\ \ddots], \qquad [\{\psi_1\}\{\psi_2\}, \ldots, \{\psi\}_r, \ldots, \{\psi_N\}], \tag{3, 4}$$

where $\overline{\omega}_r^2$ is the r_{h} eigenvalue, or natural frequency squared and $\{\psi\}_r$ is the corresponding mode shape. There two matrices contain a full description of the dynamic characteristics of the system.

The characteristic equation (2) can be pre-multiplied by $[\mathbf{M}]^{-1}$ to obtain

$$([\mathbf{A}] - \omega^2[\mathbf{I}])[\mathbf{X}] = \{0\}, \tag{5}$$

where $[\mathbf{A}] = [\mathbf{M}]^{-1}[\mathbf{K}]$ and $[\mathbf{I}]$ is the identity matrix. Here, $[\mathbf{A}]$ represents all physical parameters of the undamped system. This matrix can be transformed into wavelet space as

$$[\tilde{\mathbf{A}}] = W^{\mathrm{T}}[A]W, \tag{6}$$

where W represents the one-dimensional wavelet transform operator and W^{T} its transpose. Simply, the rows $\{b(n)\}$ and columns $\{c(n)\}$ of matrix $[\mathbf{A}]$ are expanded using the orthogonal wavelet transform as

$$\{b(n)\} = \sum_i \sum_j a_{j,i}\psi_{j,i}(t), \qquad \{c(n)\} = \sum_k \sum_l a_{l,k}\psi_{l,k}(t), \tag{7, 8}$$

where i, j, k and l are integer indices and the $\psi(t)$ are the wavelet expansion functions that form an orthogonal basis. Orthogonal basis-generating wavelets can be constructed using Mallat's algorithm given in reference [7]. There exist a number of wavelet functions, which can be used for the orthogonal expansion. The well-known Daubechies wavelets [8] are applied in this paper as an example. However, the properties of the wavelet transform used are independent of the type of wavelet function implemented [8–11]. For more details regarding wavelet analysis the reader is referred to reference [9].

The orthogonal wavelet transform in equation (6) allows one to obtain the *sparse* expansion of matrix $[\mathbf{A}]$ in which the wavelet coefficients can be severely truncated. This property has previously been used for compression of vibration data, feature

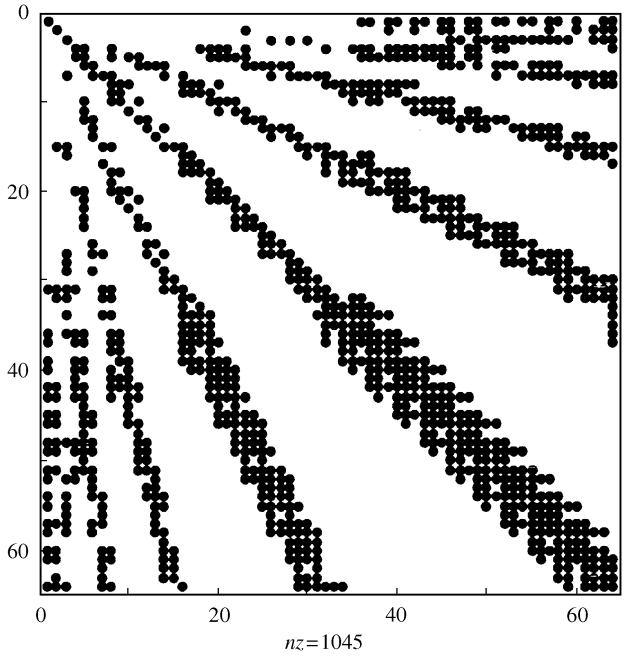

Figure 1. Wavelet transform of a (64×64) [**A**] matrix, represented graphically.

extraction/selection [10, 11] and chaos/noise analysis [12]. The *sparse* expansion can also be utilized for model reduction, which can be achieved by keeping all wavelet coefficients of the system matrix [**A**] larger than some threshold and setting all smaller coefficients to zero. Figure 1 gives an example of graphical representation of the two-dimensional wavelet transform in equation (6). It is clear here that the matrix becomes sparse in the wavelet domain. The structural model reduction based on the orthogonal wavelet transform can be implemented by reducing the matrix $[\tilde{\mathbf{A}}]$ using different thresholds and then building up a new model from the reduced wavelet matrix by the inverse of the wavelet transform. The threshold can be adjusted to vary the fraction of preserved expansion coefficients. The important fact is that after thresholding, the new model can quite accurately represent the original matrix [**A**]. Note that this kind of threshold makes the matrix *sparse*, but does not change the size of the original matrix. It is also very important in this application that the matrix in wavelet space is truncated according to the amplitude of the components, not their position in the matrix. The thresholding in this approach preserves the high-frequency components of the original model. This is because the maximum values are mainly located on the main diagonal. Figure 2 shows an example of how the full model matrix [**A**] can be reconstructed by only 307, rather than 1024, of its wavelet coefficients. Here, the amplitude and the position of the elements in each matrix $[\mathbf{A}]_W$ are represented as three-dimensional plots.

Following equation (5), the new model matrix $[\mathbf{A}]_W$ can be then used to represent the structure as

$$([\mathbf{A}]_W - \omega_W^2[\mathbf{I}])\{X\} = \{0\} \tag{9}$$

for which the only non-trivial solutions are those satisfying the condition

$$\det|[\mathbf{A}]_W - \omega_W^2[\mathbf{I}]| = 0. \tag{10}$$

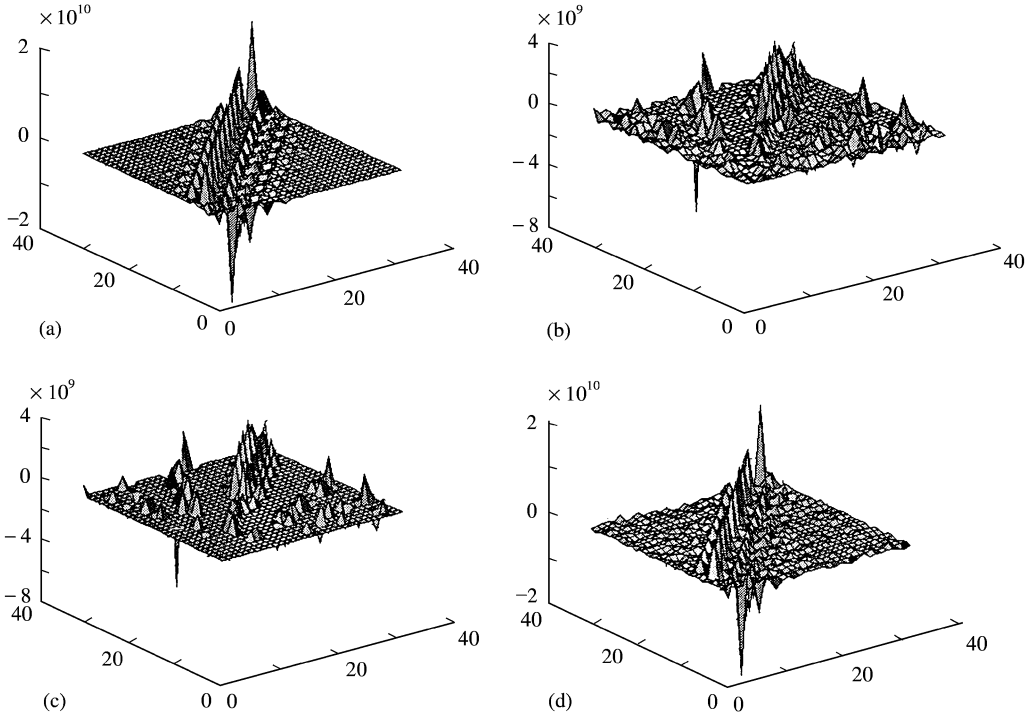

Figure 2. Graphical representation of using the orthogonal wavelet transform in model reduction: (a) graphical representation of the full model matrix $[\mathbf{A}]$ (32×32); (b) the model is transformed into the wavelet basis (32×32), which has 1024 coefficients; (c) the wavelet transform is reduced to 307 coefficients; 70% of 1024 coefficients are set to zero and (d) the new full model $[\mathbf{A}]_W$ (32×32) is then reconstructed from the remaining 30%.

This yields N possible positive real solutions $(\varpi_{W1}^2, \varpi_{W2}^2, \ldots, \varpi_{Wr}^2, \ldots, \varpi_{WN}^2)$, which are the approximated undamped natural frequencies of the analyzed system obtained from the new model matrix $[\mathbf{A}]_W$.

The size of the wavelet coefficients, $a_{j,k}$, drops off rapidly with j and k for large matrices. This means that most of the wavelet coefficients for a large model matrix are small and close to zero. The new model can then be reconstructed using a small number of its wavelet coefficients. This property enhances the use of the wavelet transform in model reduction for larger structure by deleting all small coefficients. The wavelet expansion also allows for a more accurate local description and separation of the model characteristics.

3. APPLICATION EXAMPLES

The application of the orthogonal wavelet transform method is illustrated using two simple examples. There are a 32-d.o.f. simply supported beam and a 105-d.o.f. framework structure. The modal assurance criterion (MAC) is used to compare the similarity between the reduced model $[\mathbf{A}]_W$ obtained by orthogonal wavelet transform and the full model $[\mathbf{A}]$. The MAC is defined here as

$$MAC(\{\psi_W\}_i, \{\psi\}_j) = |\{\psi_W\}_i^{\mathrm{T}}\{\psi\}_j|^2 / (\{\psi_W\}_i^{\mathrm{T}}\{\psi_W\}_i)(\{\psi\}_j^{\mathrm{T}}\{\psi\}_j), \tag{11}$$

where $\{\psi_W\}_i$ and $\{\psi\}_j$ are the reduced model and the full model mode shape vectors respectively. It gives clearer indication of modal correlation and is real and bounded

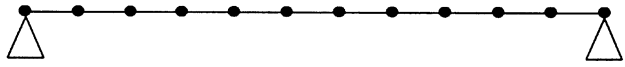

Figure 3. Simply supported beam.

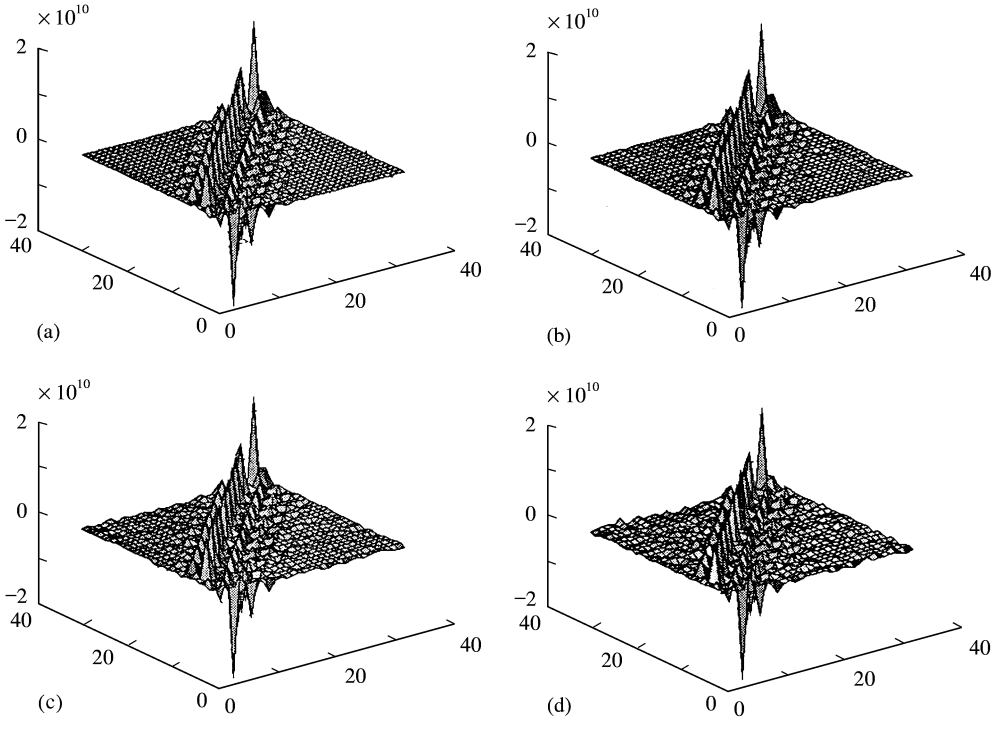

Figure 4. Different models of the simply supported beam obtained using different thresholds: (a) the full model matrix; (b) the model reconstructed from 60%; (c) the model reconstructed from 45% and (d) the model reconstructed from 30% of the wavelet coefficients.

between 0 and 1. Arbitrarily scaled reduced and full modes $\{\psi_W\}_i$ and $\{\psi\}_j$ are similar, or correlated, if their MAC value is close to 1 and uncorrelated if the MAC value is small.

3.1. SIMPLY SUPPORTED BEAM

The first structure considered is a 0·05 m thick and 2·2 m long steel simply supported 32-d.o.f. beam shown in Figure 3. The full model matrix [**A**] is of size (32 × 32), which means the structure has 32 natural frequencies. The wavelet transform of matrix [**A**] was calculated and different thresholds were applied to the wavelet coefficients. Each thresholding resulted in a new model, as shown in Figure 4. Each of these new models gives different approximations for the natural frequencies at different modes. Figure 5 shows a plot of the MAC values against different modes for the 35% reduced model. Modes, which have MAC values greater than 0·7 are considered at different thresholds. Tables 1 and 2 show the natural frequencies obtained by two different threshold levels; here each threshold converges to different modes at higher MAC values. The results of the three

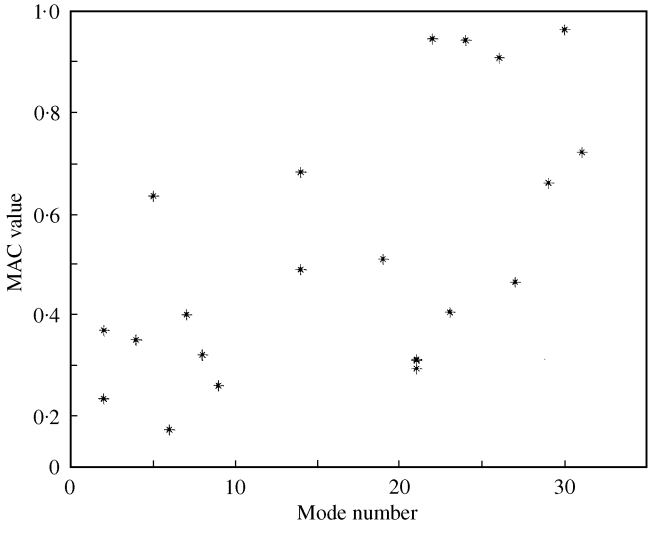

Figure 5. *MAC* values against mode number for 35% reduced model of the beam.

TABLE 1

Results of 60% *reduced model for threshold of* $[\tilde{\mathbf{A}}] > 0{\cdot}02 * max\ coefficient$

Highest *MAC* no.	Mode number	Full model ($f \times 10^4$ Hz)	Reduced model ($f \times 10^4$ Hz)	Error (%)
0·7053	32	1·4959	1·4810	0·9945
0·7746	18	0·5418	0·6211	14·6504
0·9176	22	0·7931	0·7967	0·4466
0·9748	19	0·6400	0·6323	1·1991
0·9775	24	0·9559	0·9489	0·7310
0·9918	28	1·2749	1·2709	0·3167
0·9966	30	1·3880	1·3765	0·8237
0·9973	26	1·1218	1·1267	0·4377

TABLE 2

Results of 36% *reduced model for threshold of* $[\tilde{\mathbf{A}}] > 0{\cdot}06 * max\ coefficient$

Highest *MAC* no.	Mode number	Full model ($f \times 10^4$ Hz)	Reduced model ($f \times 10^4$ Hz)	Error (%)
0·7413	26	1·1218	1·1463	2·1796
0·7714	24	0·9559	0·9917	3·7464
0·8506	28	1·2749	1·2542	1·6232
0·9213	30	1·3880	1·3300	4·1794

common modes obtained by the different threshold levels are compared in Table 3. The frequency response function (FRF) for the full model and the 40% reduced model is shown in Figure 6.

TABLE 3

Comparing the results of the three modes at four different thresholds

Mode number	Full model ($f \times 10^4$ Hz)	30% red. model	36% red. model	45% red. model	60% red. model
26	1·1218	1·1546 (2·92%)	1·1463 (2·18%)	1·1353 (1·20%)	1·1267 (0·44%)
28	1·2749	1·2127 (4·88%)	1·2542 (1·62%)	1·2591 (1·24%)	1·2709 (0·32%)
30	1·3880	1·3061 (5·90%)	1·3300 (4·18%)	1·3428 (3·25%)	1·3765 (0·82%)

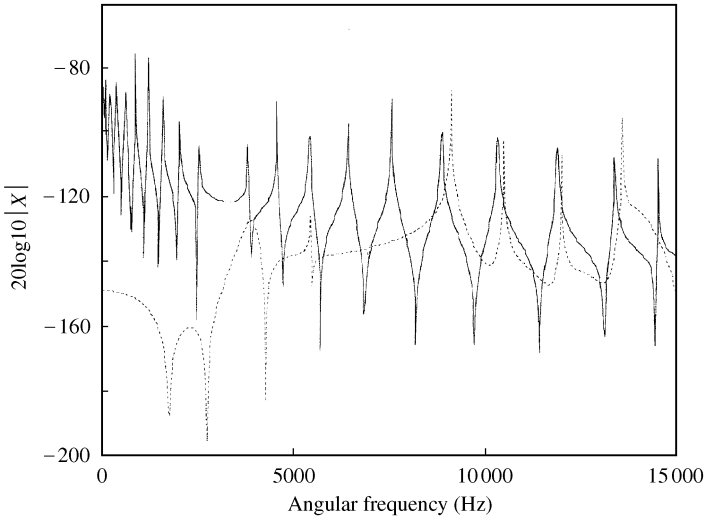

Figure 6. FRF for full model and 40% reduced model for the simply supported beam: ——, full model; ·····, 40% reduced model.

3.2. FRAMEWORK STRUCTURE

The second example considered was a steel framework of 7 m height and 4 m wide as shown in Figure 7. The framework model matrix [**A**] was of the size (105×105), which is not an integer power of 2; $(2^{n1} \times 2^{n2})$. Since the orthogonal wavelet transform computation is based on the FFT, it can only be found for a model matrix of size $(2^{n1} \times 2^{n2})$, zeros are added in rows and columns to make the model matrix [**A**] to the nearest size of $(2^{n1} \times 2^{n2})$ which is (128×128). The wavelet transform of the matrix is then found and different threshold levels are applied. When the new model is reconstructed from the reduced wavelet basis, the rows and columns of the zeros are removed to regain the size of the full model. Figure 8 shows a plot of the *MAC* values against different modes for the 30% reduced model. Modes, which have *MAC* values greater than 0·7, are considered at different threshold levels. Tables 4–6 show the results of the approximated frequencies using different threshold levels. The frequencies of the last five modes are compared for different thresholds in Table 7. The FRF for the last frequencies for the full mode and the 40% reduced model is shown in Figure 9.

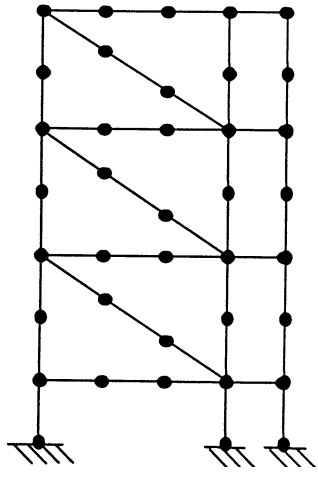

Figure 7. Framework has 38 nodes of three d.o.f.s each and it is clamped at its three ends, which results in an 105-d.o.f. structure.

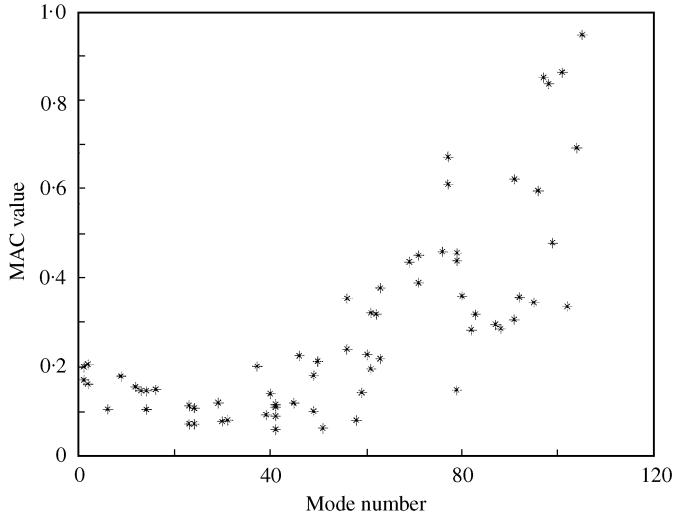

Figure 8. *MAC* values against different modes for 30% reduced model of the framework.

TABLE 4

Results of 30% *reduced model for threshold of* $[\tilde{\mathbf{A}}] > 0{\cdot}005 * max\ coefficient$

Highest *MAC* no.	Mode number	Full model ($f \times 10^3$ Hz)	Reduced model ($f \times 10^3$ Hz)	Error (%)
0·7256	102	2·3973	2·3146	3·4511
0·8377	98	2·1577	2·1547	0·1374
0·8520	97	2·0768	2·0284	2·3320
0·8642	101	2·3486	2·3146	1·4466
0·9511	105	2·6378	2·6410	0·1227

TABLE 5

Results of 20% *reduced model for threshold of* $[\tilde{\mathbf{A}}] > 0{\cdot}01 * max\ coefficient$

Highest *MAC* no.	Mode number	Full model ($f \times 10^3$ Hz)	Reduced model ($f \times 10^3$ Hz)	Error (%)
0·7049	103	2·4199	2·3974	0·9315
0·7822	104	2·6313	2·6585	1·0342
0·8349	105	2·6378	2·6156	0·8417
0·9198	102	2·3973	2·4249	1·1513
0·9475	101	2·3486	2·3399	0·3686

TABLE 6

Results of 15% *reduced model for threshold of* $[\tilde{\mathbf{A}}] > 0{\cdot}016 * max\ coefficient$

Highest *MAC* no.	Mode number	Full model ($f \times 10^3$ Hz)	Reduced model ($f \times 10^3$ Hz)	Error (%)
0·7390	104	2·6313	2·6735	1·6041
0·8021	102	2·3973	2·4028	0·2276
0·8214	103	2·4199	2·3493	2·9174
0·8658	101	2·3486	2·2621	3·6813
0·9460	105	2·6378	2·5820	2·1166

TABLE 7

Comparing the results of the last five modes at different thresholds

Mode number	Full model ($f \times 10^3$ Hz)	13% red. model	15% red. model	20% red. model	25% red. model	44% red. model
101	2·3486	2·3108 (1·61%)	2·2621 (3·68%)	2·3399 (0·37%)	2·3111 (1·59%)	2·3361 (0·53%)
102	2·3973	2·4143 (0·71%)	2·4028 (0·23%)	2·4249 (1·15%)	2·3111 (3·59%)	2·3952 (0·09%)
103	2·4199	2·3404 (3·29%)	2·3493 (2·92%)	2·3974 (0·93%)	2·4167 (0·13%)	2·4168 (0·13%)
104	2·6313	2·6425 (0·42%)	2·6735 (1·60%)	2·6585 (1·03%)	2·7007 (2·63%)	2·6436 (0·47%)
105	2·6378	2·5209 (4·43%)	2·5820 (2·12%)	2·6156 (0·84%)	2·6397 (0·07%)	2·6268 (0·42%)

4. DISCUSSION

From the results obtained for both the simply supported beam and the framework structure, it is clear that there is a high correlation between the frequencies of the reduced model and the full model at higher modes. Figures 5 and 8 show that *MAC* values are close to unity at higher modes, whereas they are small and close to zero at the first modes.

Figures 6 and 9 show that the FRF peaks for the full model and the reduced model are close at higher frequencies and thus at higher modes. This means that, in contrast to other

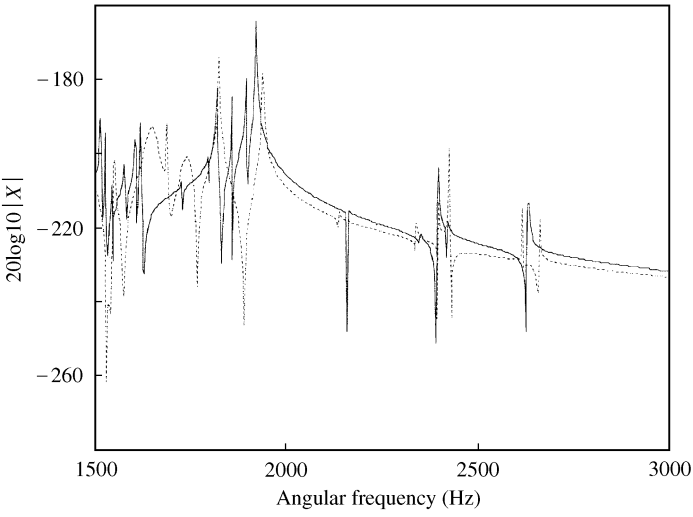

Figure 9. FRF for full model and 20% reduced model for the framework: ——, full model; ·····, reduced model.

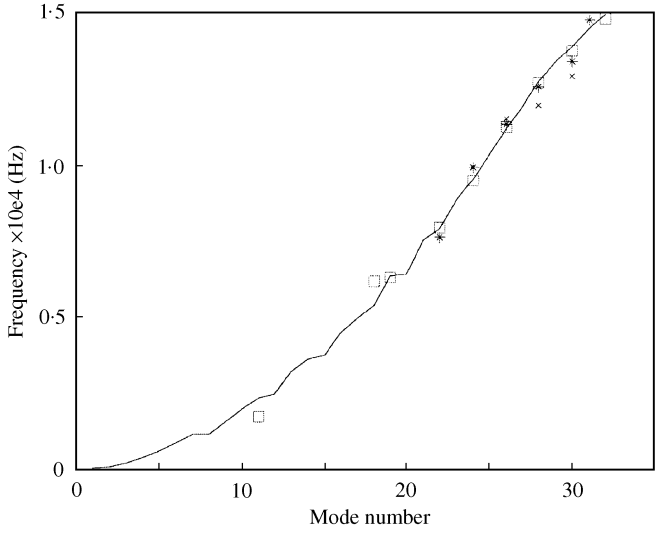

Figure 10. Comparing the frequencies obtained using different thresholds with that of the full model for the simply supported beam: ——, full model; □, 60% reduced model; ∗, 45% reduced model; ×, 30% reduced model.

model reduction techniques, the orthogonal wavelet transform converges better for higher mode frequencies.

The error associated with the reduced model based on the orthogonal wavelet transform at different threshold levels is in general (see Figures 10 and 11). Figure 11 shows closer agreement between the full and reduced model frequencies for the framework at smaller models than that shown on Figure 10 for the simply supported beam. Table 3 and 7 show that the maximum error of the approximated frequencies using the orthogonal wavelet transform for the simply supported beam and the framework are 5·90 and 4·43% respectively. Each threshold level results in a different approximation for different modes at

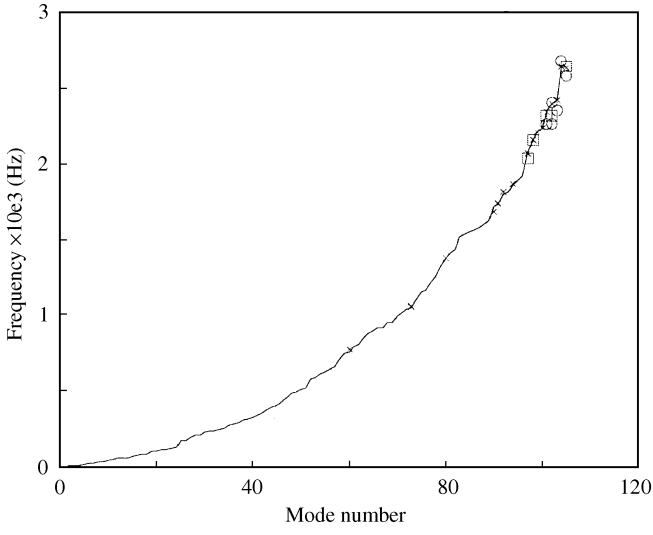

Figure 11. Comparing the results obtained using different thresholds with that of the full model for the framework: ——, full model; ×, 44% reduced model; □, 30% reduced model; ○, 15% reduced model.

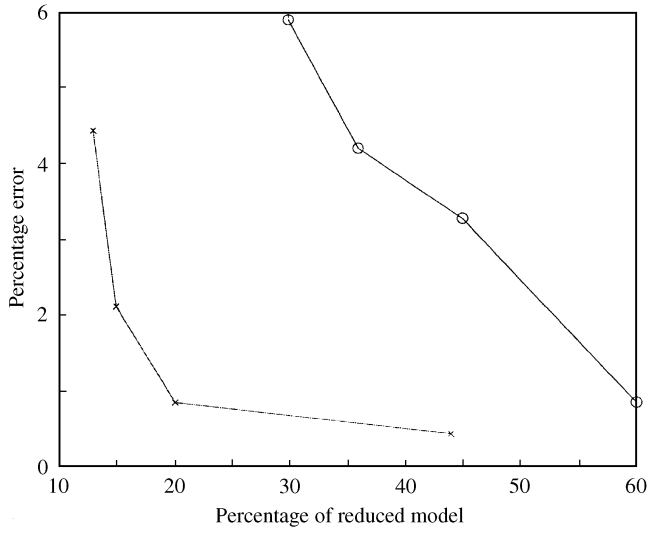

Figure 12. Error at different thresholds for two modes in the beam and the framework: —○—, $f(30)$ beam; $f(105)$ framework.

higher MAC values, as shown in Tables 1, 2 and 4–6. Comparing the results in Tables 3 and 8 for the same modes at different threshold levels it will be observed that the error decreases as the model gets larger. This is a consequence of retaining more coefficients in the wavelet basis of the model, which represent more dynamic characteristics of the structure. Figure 12 gives a comparison between the error obtained at different threshold levels for modes 30 and 105 of the simply supported beam and the framework structure respectively. It can be seen that the results for the framework structure converge more accurately to the full model at smaller models than that for the simply supported beam.

One property of the orthogonal wavelet transform is the drop in the size of the wavelet coefficients $a_{j,k}$ for a large class of matrix. This means that, for a large model matrix, many wavelet coefficients are small and close to zero. This in turn leads to higher reduction in the wavelet basis of the model and a new model can be reconstructed using a smaller number of its wavelet coefficients. Therefore, the orthogonal wavelet transform performs better for larger structures than for small ones. This is clear when the comparison between the results for the (32×32) simply supported beam model and the (105×105) framework structure model are made. Table 3 shows that the maximum reduction for the wavelet basis of the simply supported beam model is 30%, which has a maximum error of 5·90% for mode 30. On the other hand, Table 7 shows that the maximum reduction for the framework is 13% giving a maximum error of 4·43% for mode 105.

5. CONCLUSIONS

The orthogonal wavelet transform has been used for model reduction of structures. The method has been illustrated using a simply supported beam and a framework structure. The method preserves higher mode frequencies more accurately than lower mode frequencies. Comparing the results for the framework and the beam, the orthogonal wavelet transform converges more accurately to the full model at smaller models for larger structures than that for small structures (i.e., 13% reduced model for the framework and 30% reduced model for the simply supported beam). The error in predicting the frequencies at higher modes is not significant for the reduced model using the orthogonal wavelet transform. The maximum errors obtained were 5·90% for the simply supported beam and 4·43% for the framework.

In summary, the orthogonal wavelet transform shows the potential for modal reduction of structures. However, more investigations are required to confirm the findings. The future work should involve the thresholding procedure based on the position and/or amplitude of wavelet coefficients. This will improve the convergence for lower mode frequencies. Also, it is important to find the correlation between wavelet coefficients and the degrees of freedom of the numerical models for engineering application of the proposed method.

ACKNOWLEDGMENT

The authors would like to thank Dr. Graeme Manson from the Dynamics Research Group for his useful suggestions and discussions on the topic.

REFERENCES

1. R. J. GUYAN 1965 *American Institute of Aeronautics and Astronautics Journal* **3**, 380. Reduction of stiffness and mass matrices.
2. M. I. FRISWELL, S. D. GARVEY and J. E. T. PENNY 1995 *Journal of Sound and Vibration* **186**, 311–323. Model reduction using dynamic and iterated IRS techniques.
3. C. A. MILLER 1980 *American Society of Civil Engineers Journal of the Structural Division* **106**, 2091–2109. Dynamic reduction of structural models.
4. J. O'CALLAHAN 1989 *Proceedings of the 7th International Modal Analysis Conference, Las Vegas*, 17–21. A procedure for an improved reduced system (IRS) model.
5. J. O'CALLAHAN, P. AVITABILE and R. RIEMER 1989 *Proceedings of the 7th International Modal Analysis Conference, Las Vegas, January*, 29–37. System equivalent reduction expansion process (SEREP).
6. F. SCARPA and G. TOMLISON 2000 *Journal of Sound and Vibration* **230**, 45–67. Theoretical characteristics of the vibration of sandwich plates with in-plane negative Poisson's ratio values.

7. S. G. MALLAT 1989 *IEEE Transactions on Pattern Recognition and Machine Intelligence* **11**, 674–693. A theory for multiresolution signal decomposition: the wavelet representation.
8. I. DAUBECHIES 1992 *Ten Lectures on Wavelets*. Philadelphia, PA: SIAM.
9. S. MALLAT 1998 *A Wavelet Tour of Signal Processing*. San Diego: Academic Press.
10. W. J. STASZEWSKI 2000 *Wavelets for Mechanical and Structural Damage Identification*. Gdansk: Polish Academy of Sciences Press, Institute of Fluid-Flow Machinery.
11. W. J. STASZEWSKI 1998 *Journal of Sound and Vibration* **211**, 735–760. Wavelet data compression and feature selection for vibration analysis.
12. W. J. STASZEWSKI and K. WORDEN 1998 *Special Issue of the International Journal of Bifurcation and Chaos* **9**, 455–471. Wavelet analysis of time series: coherent structures, chaos and noise.